

## Analysis of intracranial pressure pulse waveform in traumatic brain injury patients: a CENTER-TBI study

Agnieszka Uryga, PhD,<sup>1</sup> Arkadiusz Ziółkowski, MSc,<sup>1</sup> Agnieszka Kazimierska, MSc,<sup>1</sup> Agata Pudełko, MSc,<sup>1</sup> Cyprian Mataczyński, MSc,<sup>2</sup> Erhard W. Lang, MD, PhD,<sup>3,4</sup> Marek Czosnyka, PhD,<sup>5,6</sup> Magdalena Kasprowicz, PhD,<sup>1</sup> and the CENTER-TBI High-Resolution ICU (HR ICU) Sub-Study Participants and Investigators

<sup>1</sup>Department of Biomedical Engineering, Faculty of Fundamental Problems of Technology, Wrocław University of Science and Technology, Wrocław, Poland; <sup>2</sup>Department of Computer Engineering, Faculty of Information and Communication Technology, Wrocław University of Science and Technology, Wrocław, Poland; <sup>3</sup>Neurosurgical Associates, Red Cross Hospital, Kassel, Germany; <sup>4</sup>Department of Neurosurgery, Faculty of Medicine, Georg-August-Universität, Göttingen, Germany; <sup>5</sup>Brain Physics Laboratory, Department of Clinical Neurosciences, Division of Neurosurgery, Addenbrooke's Hospital, University of Cambridge, Cambridge, United Kingdom; and <sup>6</sup>Institute of Electronic Systems, Faculty of Electronics and Information Technology, Warsaw University of Technology, Warsaw, Poland

**OBJECTIVE** Intracranial pressure (ICP) pulse waveform analysis may provide valuable information about cerebrospinal pressure-volume compensation in patients with traumatic brain injury (TBI). The authors applied spectral methods to analyze ICP waveforms in terms of the pulse amplitude of ICP (AMP), high frequency centroid (HFC), and higher harmonics centroid (HHC) and also used a morphological classification approach to assess changes in the shape of ICP pulse waveforms using the pulse shape index (PSI).

**METHODS** The authors included 184 patients from the Collaborative European NeuroTrauma Effectiveness Research in Traumatic Brain Injury (CENTER-TBI) High-Resolution Sub-Study in the analysis. HFC was calculated as the average power-weighted frequency within the 4- to 15-Hz frequency range of the ICP power density spectrum. HHC was defined as the center of mass of the ICP pulse waveform harmonics from the 2nd to the 10th. PSI was defined as the weighted sum of artificial intelligence-based ICP pulse class numbers from 1 (normal pulse waveform) to 4 (pathological waveform).

**RESULTS** AMP and PSI increased linearly with mean ICP. HFC increased proportionally to ICP until the upper breakpoint (average ICP of 31 mm Hg), whereas HHC slightly increased with ICP and then decreased significantly when ICP exceeded 25 mm Hg. AMP ( $p < 0.001$ ), HFC ( $p = 0.003$ ), and PSI ( $p < 0.001$ ) were significantly greater in patients who died than in patients who survived. Among those patients with low ICP ( $< 15$  mm Hg), AMP, PSI, and HFC were greater in those with poor outcome than in those with good outcome (all  $p < 0.001$ ).

**CONCLUSIONS** Whereas HFC, AMP, and PSI could be used as predictors of mortality, HHC may potentially serve as an early warning sign of intracranial hypertension. Elevated HFC, AMP, and PSI were associated with poor outcome in TBI patients with low ICP.

<https://thejns.org/doi/abs/10.3171/2022.10.JNS221523>

**KEYWORDS** intracranial pressure; pulse amplitude; pulse shape index; clinical outcome; spectral analysis; morphological analysis; traumatic brain injury

**I**NTRACRANIAL pressure (ICP) is commonly monitored in neurocritical care units. Even though it is a very complex signal that contains different subcomponents, mean ICP is usually used to guide the management of traumatic brain injury (TBI) patients. While assessment of

mean ICP may be useful in cerebral perfusion pressure-oriented therapy,<sup>1</sup> analysis of the ICP waveform (both slow and fast ICP changes) may provide valuable additional information regarding cerebral autoregulation,<sup>2</sup> cerebral hemodynamics,<sup>3</sup> cerebrospinal fluid circulation,<sup>4</sup> and the

**ABBREVIATIONS** AIS = Abbreviated Injury Scale; AMP = pulse amplitude of ICP; AU = arbitrary units; AUC = area under the curve; CENTER-TBI = Collaborative European NeuroTrauma Effectiveness Research in Traumatic Brain Injury; CT = computed tomography; FFT = fast Fourier transform; GCS = Glasgow Coma Scale; GOSE = Glasgow Outcome Scale Extended; HFC = high frequency centroid; HHC = higher harmonics centroid; ICP = intracranial pressure; ICU = intensive care unit; IQR = interquartile range; ISS = Injury Severity Score; MANOVA = multivariate analysis of variance; MLS = midline shift; PRx = pressure reactivity index; PSI = pulse shape index; ResNet = Residual Neural Network; ROC = receiver operator characteristic; TBI = traumatic brain injury.

**SUBMITTED** June 27, 2022. **ACCEPTED** October 28, 2022.

**INCLUDE WHEN CITING** Published online December 23, 2022; DOI: 10.3171/2022.10.JNS221523.

state of cerebrospinal compliance.<sup>5</sup> Regarding the latter, analysis of the shape of the cardiac-induced ICP pulse waveforms that naturally occur in the ICP signal seems to be of particular importance.<sup>6</sup>

Among the parameters that describe the shape of the ICP pulse, pulse amplitude of ICP (AMP) is one of the most frequently studied. The relationship between AMP and mean ICP in terms of the amplitude–pressure characteristic<sup>7</sup> and the RAP index<sup>8</sup> has been the subject of many studies that have presented the correlations of these metrics with outcome in TBI patients.<sup>9,10</sup>

Another ICP pulse shape–derived index is high frequency centroid (HFC). HFC describes changes in the shape of the ICP pulse by means of analysis of its frequency content. HFC was suggested as a measure of intracranial compliance and increased value was shown to be associated with mortality after TBI.<sup>11</sup> A different centroid metric—higher harmonics centroid (HHC)—was proposed to provide a measure that is less dependent on heart rate than HFC. However, this index was mainly investigated in hydrocephalus.<sup>12</sup> The results of a single study performed in TBI patients showed that HHC is lower during ICP plateau waves compared with the whole monitoring period and that a breakpoint in the mean ICP-HHC characteristic exists.<sup>13</sup>

Spectral signal processing techniques are used to determine AMP, HFC, and HHC. However, the variability of the ICP pulse shape over time and its potential nonlinear dependence on mean ICP and cerebrospinal compliance make frequency domain analysis difficult to interpret. A promising alternative is presented by time domain approaches that incorporate machine learning techniques, which have been gaining more and more popularity in medicine. Recently, we proposed a new approach for ICP pulse analysis that uses an artificial neural network.<sup>14</sup> We developed a novel metric—the pulse shape index (PSI)—based on morphological classification of ICP pulse waveforms into 4 different classes ranging from normal to pathological. The results of our study showed that classification of ICP pulse shapes can be done in real time and that TBI patients with fatal outcomes exhibit pathological waveforms more frequently than those who survived, even those with relatively low mean ICP.<sup>15</sup>

Despite the variety of indices proposed to describe the ICP pulse shape, their meaning and interpretation have not been investigated in detail or fully understood. The factors that influence the shape of pulse ICP (i.e., changes in cerebral blood volume, arterial inflow, venous outflow, and mean ICP<sup>16</sup>) may potentially have a different impact on their values, and their clinical and predictive usefulness may also differ. To address this issue, here we studied the relationships between ICP pulse waveform–derived metrics (AMP, HFC, HHC, and PSI) in a multicenter database of TBI patients. Additionally, we assessed the link between these parameters and mean ICP. Finally, the clinical significance of all analyzed metrics was evaluated by studying their relationship with the presence of midline shift (MLS) in computed tomography (CT) scans and their association with mortality and outcome in patients with TBI.

## Methods

### Study Population

We analyzed data from the cohort of TBI patients enrolled in the Collaborative European NeuroTrauma Effectiveness Research in Traumatic Brain Injury (CENTER-TBI) project. CENTER-TBI was a large multicenter European project that aimed to better understand and improve the care of patients with TBI (Appendix). The project's primary objectives included the collection of high-quality clinical and epidemiological data, multidimensional characterization of TBI as a disease, identification of the most effective clinical interventions for TBI management, and development of novel tools for prediction of outcome. Patients were recruited prospectively between the beginning of 2015 and the end of 2017 from 21 medical centers across Europe. All patients were treated according to the current evidence-based guidelines for TBI.<sup>17</sup> Detailed information on data collection is available on the study website (<https://www.center-tbi.eu/data/dictionary>).

In this study, a subgroup of patients named the High-Resolution Sub-Study, which had high-frequency digital signal recordings from intensive care unit (ICU) monitoring (full waveform resolution with sampling frequencies of at least 100 Hz), was analyzed. Patients older than 16 years of age and with 6-month Glasgow Outcome Scale Extended (GOSE) scores available were included in the final analysis. Patients who underwent decompressive craniectomy before the start of ICP monitoring or external ventricular drain placement were excluded because craniectomy significantly changes the intracranial pressure–volume relationship (due to the removal of part of the skull boundary), whereas external ventricular drainage makes the analysis of ICP pulse waveforms impossible when the system is open for cerebrospinal fluid drainage. The study design flowchart is presented in Supplementary Fig. 1.

### Ethical Approval

The CENTER-TBI study (European Commission [EC] grant 602150) has been conducted following all relevant laws of the European Union (EU) if directly applicable or of direct effect and all relevant laws of the country where the recruiting sites were located, including but not limited to, the relevant privacy and data protection laws and regulations (the “Privacy Law”), the relevant laws and regulations on the use of human materials, and all relevant guidance relating to clinical studies from time to time in force, including but not limited to, the International Conference on Harmonization (ICH) Harmonized Tripartite Guideline for Good Clinical Practice (CPMP/ICH/135/95; “ICH GCP”) and the World Medical Association Declaration of Helsinki entitled “Ethical Principles for Medical Research Involving Human Subjects.” Informed consent from the patients and/or the legal representative/next of kin was obtained, accordingly to local legislation, for all patients recruited in the core data set of CENTER-TBI and documented in the electronic case report form. Ethical approval was obtained for each recruiting site. The list of sites, ethical committees, approval numbers, and approval dates can be found on the study website (<https://www>).

center-tbi.eu/project/ethical-approval). The data used in this study were obtained (with permission) in the context of CENTER-TBI, a large collaborative project with the support of the European Union 7th Framework program (EC grant 602150).

### Signal Monitoring and Processing

ICP was measured using an intraparenchymal strain gauge probe (Codman ICP MicroSensor, Codman & Shurtleff, Inc.) or a parenchymal fiber-optic pressure sensor (Camino ICP Monitor, Integra Life Sciences). Arterial blood pressure was obtained through a radial or femoral arterial line connected to a pressure transducer (Baxter Healthcare Corp., CardioVascular Group). The signals were recorded with a sampling frequency of 100 Hz or higher using ICM+ software (Cambridge Enterprise Ltd.) or Moberg CNS Monitor (Moberg Research, Inc.).

The signals were preprocessed using a 2-step artifact removal procedure. In the first step, artifacts were marked on the basis of source annotations in the original HDF5 file and replaced with the median of their immediate surroundings. In the second step, a Residual Neural Network (ResNet) model was applied to detect and remove artifactual pulse waveforms from the ICP signal. Details about the ResNet model used in this study can be found in our previous paper,<sup>14</sup> and the source codes with the weights for the trained model are available in an online repository ([https://github.com/CMataczynski/ICP\\_NN](https://github.com/CMataczynski/ICP_NN)). Neural network-related calculations were performed on a machine with AMD Ryzen 9 3900XT 12 core CPU and Nvidia GeForce RTX 3090 GPU (no supercomputer was needed).

Pulse classification along with calculation of all other ICP-related parameters took on average 6 hours for the entire database of recordings. All subsequent analyses were performed on only the nonartifactual parts of the signals. Data from the day of trauma through day 7 were used to calculate mean ICP and related parameters. The mean values of all signals and derived parameters were calculated using waveform time integration over 10-second intervals. An example of the calculated indices is presented in Supplementary Fig. 2.

### Spectral Analysis

The ICP waveform (Fig. 1A) can be decomposed using fast Fourier transform (FFT) into a set of sinusoidal components with different amplitudes and frequencies (Fig. 1B). FFT produces a representation of the signal as a function of frequency, which is called the amplitude spectrum of the signal (Fig. 1C). This operation allows for oscillations of different frequencies (such as the fundamental component corresponding to the cardiac cycle) to be analyzed separately because in the time domain they are overlaid with each other.

### AMP of ICP

AMP was expressed as the amplitude of the fundamental harmonic of the ICP pulse waveform within the range containing the heart rate frequency of adult humans (40–180 bpm, corresponding to 0.67–3 Hz) by using spectral analysis based on FFT (Fig. 1D).

### High Frequency Centroid

While AMP is a measure related to only the fundamental component of the signal, the frequency centroid takes into account the distribution of the power of the ICP wave over a range of frequencies rather than in 1 main frequency. HFC is calculated from the spectral content contained within the frequency range from  $b_1 = 4$  Hz to  $b_2 = 15$  Hz (marked by the blue rectangle in Fig. 1E). Each sample within that range is characterized by frequency  $f_k$  (in hertz) corresponding to bin  $k$  and amplitude  $A_k$ . HFC is the amplitude-weighted average frequency described by Equation 1 shown below:<sup>11</sup>

$$HFC = \frac{\sum_{k=b_1}^{b_2} f_k \cdot A_k}{\sum_{k=b_1}^{b_2} A_k} \quad (1)$$

### Higher Harmonics Centroid

In contrast to HFC, HHC is not calculated from all the samples within a given frequency range but from only the harmonics numbered from  $m = 2$  to  $m = 10$  (Fig. 1F), according to Equation 2:<sup>13</sup>

$$HHC = \frac{\sum_{m=b_1}^{b_2} m \cdot A_m}{\sum_{m=b_1}^{b_2} A_m} \quad (2)$$

where  $m$  is the harmonic number,  $A_m$  is the spectral amplitude at harmonic  $m$ , and  $b_1$  and  $b_2$  are the edges (expressed in harmonic number) of the band over which the centroid is calculated.

### Pulse Shape Index

In normal intracranial conditions, the systolic peak (P1) of the ICP pulse waveform is higher than the tidal (P2) and dirotic (P3) peaks, and the dirotic notch is easy to identify. However, with decreasing intracranial compliance, P2 and P3 start to exceed P1 while the dirotic notch disappears.<sup>5,18</sup> Thus, according to Nucci et al.,<sup>19</sup> ICP pulse waveforms can be classified as 1 of 4 morphological types from normal (class 1) to pathological (class 4) (Fig. 2).

In our study, morphological classification of ICP pulses was achieved with the ResNet model that was developed and described in detail in our previous study.<sup>14</sup> In brief, the algorithm includes the following steps: 1) segmentation of ICP recordings into individual pulse waveforms using the modified Scholkmann algorithm;<sup>20</sup> 2) normalization of the obtained pulse waveforms to range 0–1; 3) unification of the length of pulse waveforms to 180 samples; and 4) ICP pulse waveform shape classification on a scale from class 1 (normal shape) to class 4 (pathological shape) using ResNet.<sup>14</sup>

The results of ICP morphological classification were used to calculate PSI, which was defined as the weighted sum of class numbers according to the following formula (Fig. 2):

$$PSI = \sum_{i=1}^4 i \cdot p_i \quad (3)$$

where  $i$  is the ICP pulse waveform class number and  $p_i$  is the percentage fraction of pulses marked as a given class

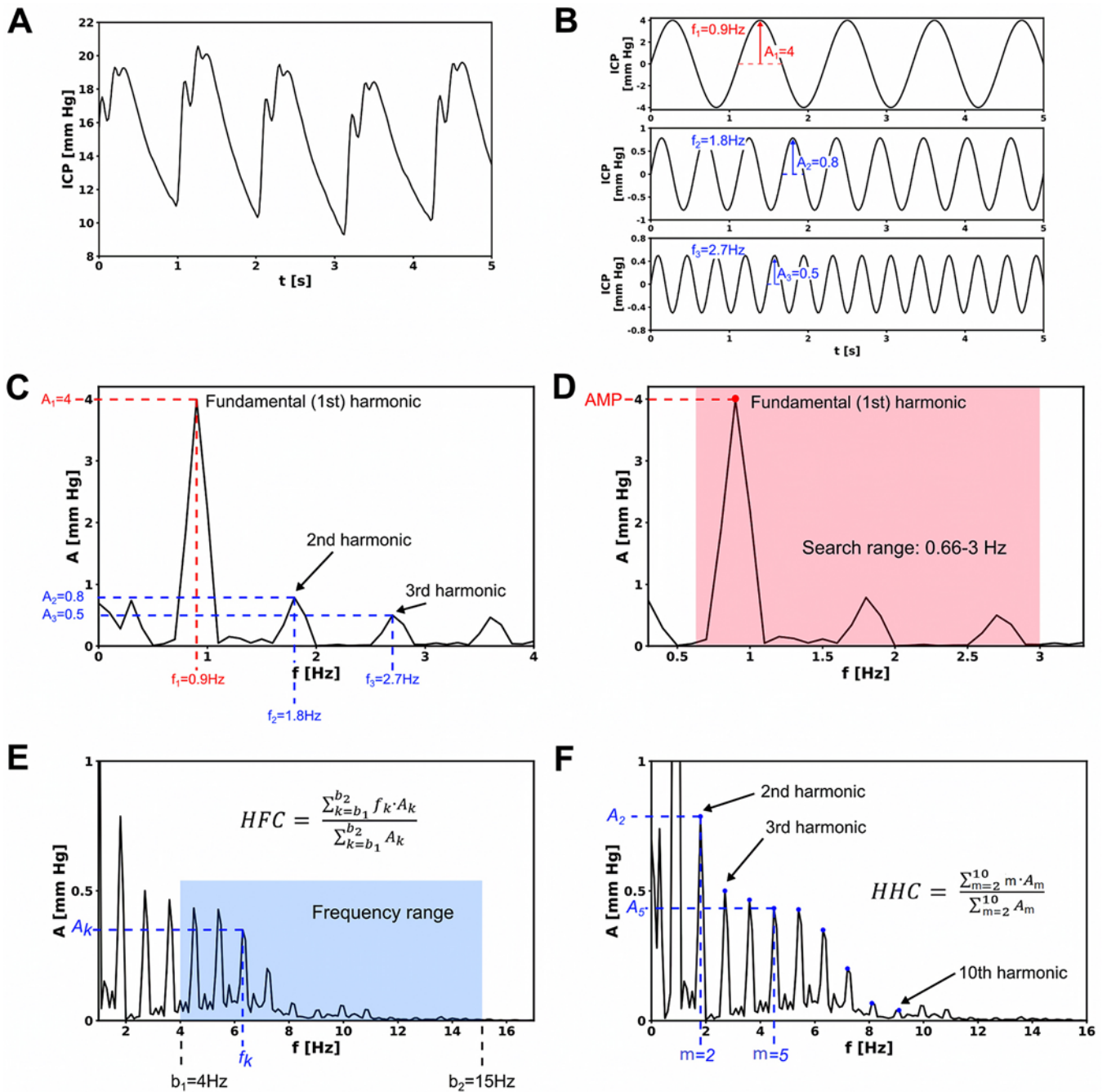


**FIG. 1.** Illustrative examples of the intermediate steps performed to obtain AMP, HFC, and HHC of the ICP signal. **A:** First, FFT breaks down the ICP waveform into a set of component sinusoidal waves with different amplitudes ( $A$ ) and frequencies ( $f$ ). **B:** The fundamental component is illustrated (i.e., the “strongest” component of the pulsatile ICP signal corresponding to heart rate [ $\mu\text{-per}$ ]), as well as specific spectral components, called harmonics, which are multiples of the fundamental frequency; here, the 2nd and 3rd harmonics are shown for illustration purposes. **C:** FFT produces a representation of the signal as a function of frequency, called the amplitude spectrum of the signal. Each of the 3 sinusoidal components from panel B is visible as a local maximum (peak). This operation allows for oscillations with different frequencies (such as the fundamental component corresponding to the cardiac cycle) to be analyzed separately; they are overlaid with each other in the time domain. **D:** AMP is calculated as the amplitude of the fundamental (1st) component by finding the maximum of the amplitude spectrum in the range corresponding to heart rate in an adult human (40–180 bpm, or 0.67–3 Hz). The maximum is marked by a red dot in the plot. **E:** HFC is calculated from the spectral content contained within the frequency range from  $b_1 = 4\text{ Hz}$  to  $b_2 = 15\text{ Hz}$  (marked by the blue rectangle). Each sample within that range is characterized by frequency  $f_k$  and amplitude  $A_k$ . HFC is the amplitude-weighted average frequency described by the equation shown in the plot. It can be likened to the center of mass of the spectrum, where mass corresponds to the amplitude of each frequency component. **F:** In contrast to HFC, HHC is not calculated from all the samples within a given frequency range, but only from the harmonics numbered from  $m = 2$  to  $m = 10$  (i.e., from 2 to 10 times the fundamental frequency). It is expressed in harmonic number rather than in hertz and is theoretically less dependent on heart rate than HFC.  $t = \text{time}$ . Figure is available in color online only.

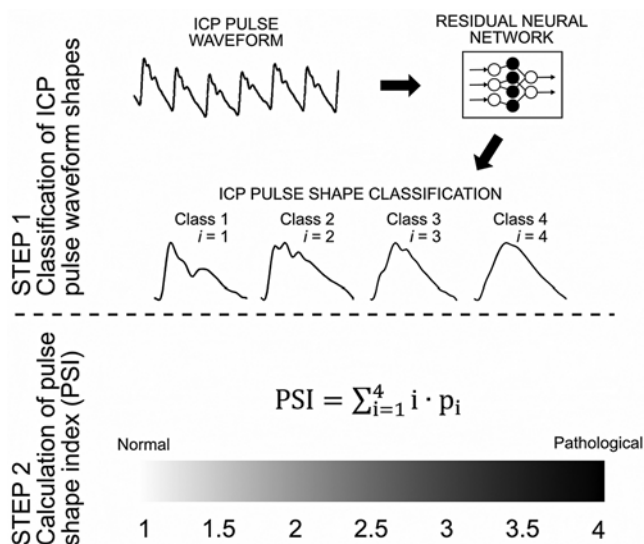


**FIG. 2.** Overview of the ICP pulse waveform classification approach. Five classes were annotated with ResNet: normal (class 1), potentially pathological (class 2), likely pathological (class 3), pathological (class 4), and artifacts. Artifactual pulses were excluded from further analysis. PSI was calculated as the weighted sum of class numbers ( $i$ ) with weights ( $p_i$ ) corresponding to the fraction of pulses assigned to given class. PSI takes values from the range between 1 (only normal waveforms of class 1) and 4 (only pathological waveforms of class 4).

in the whole analysis period (excluding artifacts). PSI was calculated in 5-minute windows with a 10-second window shift. The parameter is dimensionless (i.e., expressed in arbitrary units [AU]).

### CT Characteristics

Pathological features on CT imaging were assessed on the basis of the first head CT scan performed after admission. Patients were considered to exhibit MLS if shift > 5 mm was present. Intracerebral hemorrhage volume was estimated using the ABC/2 method.<sup>21</sup> Note that 1 patient may have had more than 1 CT abnormality in addition to MLS; in this study, additional pathologies were not analyzed.

### Mortality and Outcome

Follow-up status was assessed using GOSE scores after 6 months. The outcome was classified as poor (GOSE score 1–4) or good (GOSE score 5–8). Patients were categorized as those who survived and those who were deceased on the basis of records about in-hospital mortality and GOSE score 1 after 6 months.

### Statistical Analysis

The normality of the data was assessed using the Shapiro-Wilk test. Because the normality condition was not met for most of the analyzed parameters, nonparametric tests were applied in further analyses. The differences in median values were tested using the Mann-Whitney U-test along with estimation of effect size. Correlation analysis was performed using the Spearman's rank test.

Multivariate analysis of variance (MANOVA) was used to determine whether 2 categorical grouping variables and their interactions significantly affected the pulse ICP-derived parameters. The receiver operator characteristic (ROC) curves with area under the curve (AUC) scores were used to determine the cutoff values for AMP, HFC, and PSI and to predict mortality. The Kaplan-Meier plot and Cox proportional hazards model with FCox statistics were used to assess differences in mortality with regard to the threshold value. In survival analysis, patients who survived were classified as censored observations. The time of observation was set to the time of death (deceased cases) or a follow-up time of 180 days (surviving cases). For all tests, alpha was set to 0.05 for significance. Data are presented as median (interquartile range [IQR]) unless indicated otherwise. Statistical analysis was performed using STATISTICA 13 (Tibco).

## Results

### Patient Characteristics

The cohort consisted of 184 patients (77% men) with high-frequency digital signal recordings. The median (IQR) age was 51 (31–64) years. Detailed clinical characteristics of the group are presented in Table 1. With a median Abbreviated Injury Scale (AIS) score of 5 (4–5), median Injury Severity Score (ISS) of 34 (25–45), and median pre-ICU Glasgow Coma Scale (GCS) score of 7 (4–11), the group was classified with moderate to severe TBI. Eleven patients (6%) underwent decompressive craniectomy. The recordings from these patients were not analyzed. The median GOSE score at 6 months after injury was 4 (3–6).

### ICP Pulse Waveform–Derived Parameters Versus Mean ICP

The relationships between ICP pulse waveform–derived parameters and mean ICP are presented in Fig. 3. AMP and PSI gradually increased with ICP, and their correlations with mean ICP were significant ( $r_s = 0.40$  and  $p < 0.001$  for AMP;  $r_s = 0.22$  and  $p = 0.002$  for PSI) (Fig. 3A and B). HFC increased nonlinearly with ICP until the upper breakpoint at a mean ICP of 31 mm Hg (Fig. 3C). HHC increased slightly with ICP and then decreased significantly when ICP exceeded 25 mm Hg (Fig. 3D). The relationships between spectral indices and PSI, as well as the results of the correlation analysis between ICP pulse waveform–derived parameters, are presented in Supplementary Data.

### ICP Pulse Waveform–Derived Parameters Versus MLS

A comparison of the ICP pulse waveform–derived parameters between the groups with and without MLS is presented in Table 2. HFC, HHC, and PSI (but not AMP) were significantly greater in patients with MLS in early CT scans than in those without MLS. Supplementary Table 1 presents the results of the MANOVA performed to determine whether the presence of MLS in the early CT scans and ICP > 15 mm Hg significantly affected the parameters derived from the pulse waveforms of ICP. ICP > 15 mm Hg significantly influenced AMP, whereas MLS significantly influenced HFC, HHC, and PSI.

**TABLE 1. Baseline characteristics of all 184 patients with TBI from the CENTER-TBI database**

Characteristic	Total (n = 184)
<b>Clinical parameters</b>	
Age, yrs	51 (33)
Female	42 (23%)
<b>Cause of injury</b>	
Road traffic incident	84 (46%)
Incident fall	61 (33%)
Other nonintentional injury	5 (3%)
Violence/assault	14 (8%)
Suicide attempt	1 (1%)
Unknown	10 (5%)
Other	9 (5%)
<b>AIS grade</b>	
Grade 1	1 (1%)
Grade 2	0
Grade 3	6 (3%)
Grade 4	26 (14%)
Grade 5	150 (82%)
Grade 6	1 (1%)
ISS total	34 (20)
<b>GCS</b>	
Motor score	4 (4)
Verbal score	1 (3)
Eye score	2 (2)
<b>Pupillary reactivity at baseline</b>	
Both reacting	112 (61%)
1 reacting	4 (2%)
0 reacting	12 (7%)
NA	56 (31%)
<b>Hypoxia (pre-ICU admission)</b>	
Definite	19 (10%)
Suspect	11 (6%)
No	128 (70%)
NA	26 (14%)
<b>Hypotension (pre-ICU admission)</b>	
Definite	15 (8%)
Suspect	6 (3%)
No	137 (74%)
NA	26 (14%)
<b>CT characteristics</b>	
Cisternal compression	61 (33%)
Contusion	117 (64%)
Epidural hematoma	38 (21%)
Intraventricular hemorrhage	61 (33%)
Mass lesion	62 (35%)
MLS	39 (21%)
Skull fracture	94 (51%)
Traumatic subarachnoid hemorrhage	139 (76%)

CONTINUED IN NEXT COLUMN »

» CONTINUED FROM PREVIOUS COLUMN

**TABLE 1. Baseline characteristics of all 184 patients with TBI from the CENTER-TBI database**

Characteristic	Total (n = 184)
<b>Parameters derived from continuous monitoring</b>	
ICP, mm Hg	12.96 (6.19)
AMP, mm Hg	2.03 (1.42)
PSI, AU	2.30 (1.39)
HFC, Hz	7.29 (0.56)
HHC, harmonics no.	3.85 (0.57)
HR, bpm	74.14 (20.14)
ABP, mm Hg	83.60 (12.13)
<b>Outcome</b>	
GOSE at 6 mos	4 (3)
Grade 1 (death)	36 (20%)
Grade 2/3	47 (26%)
Grade 4	16 (9%)
Grade 5	39 (21%)
Grade 6	21 (11%)
Grade 7	12 (7%)
Grade 8	13 (7%)

ABP = arterial blood pressure; HR = heart rate; NA = not available. Continuous variables are shown as median (IQR) and categorical variables as number (%).

**ICP Pulse Waveform–Derived Parameters Versus Outcome**

A comparison of AMP, PSI, HFC, and HHC between the groups with good and poor outcomes is shown in Fig. 4. All parameters except HHC were significantly greater in patients with poor treatment outcome than patients with good treatment outcome. Moreover, in the subgroup of patients with low mean ICP (< 15 mm Hg), we found that PSI, AMP, and HFC were significantly greater in the patients with poor outcome than those with good outcome (Table 3). These differences were not seen in the subgroup with high mean ICP. No differences in HHC were found between the poor and good outcome groups, regardless of whether the low or elevated ICP range was analyzed.

**Survival Analysis**

AMP was significantly greater in patients who died (median [IQR] 3.02 [2.04–4.02] mm Hg) than those who survived (1.85 [1.34–2.42] mm Hg) (p < 0.001), with moderate effect size (r = 0.33). AMP was a significant predictor of mortality (AMP cutoff value 2.48 mm Hg, AUC = 0.77, p < 0.001). Based on the Kaplan-Meier survival analysis, AMP > 2.48 mm Hg increased the risk of death (F = 5.99, p < 0.001) (Fig. 5A).

HFC was significantly greater in patients who died (median [IQR] 7.53 [7.24–7.82] Hz) than those who survived (7.25 [7.01–7.53] Hz, p = 0.003), with small effect size (r = 0.22). Analysis of the ROC curve showed that HFC was a good predictor of mortality (HFC cutoff value 7.60 Hz, AUC = 0.66, p = 0.003). Kaplan-Meier survival analysis confirmed that the risk of death was significantly

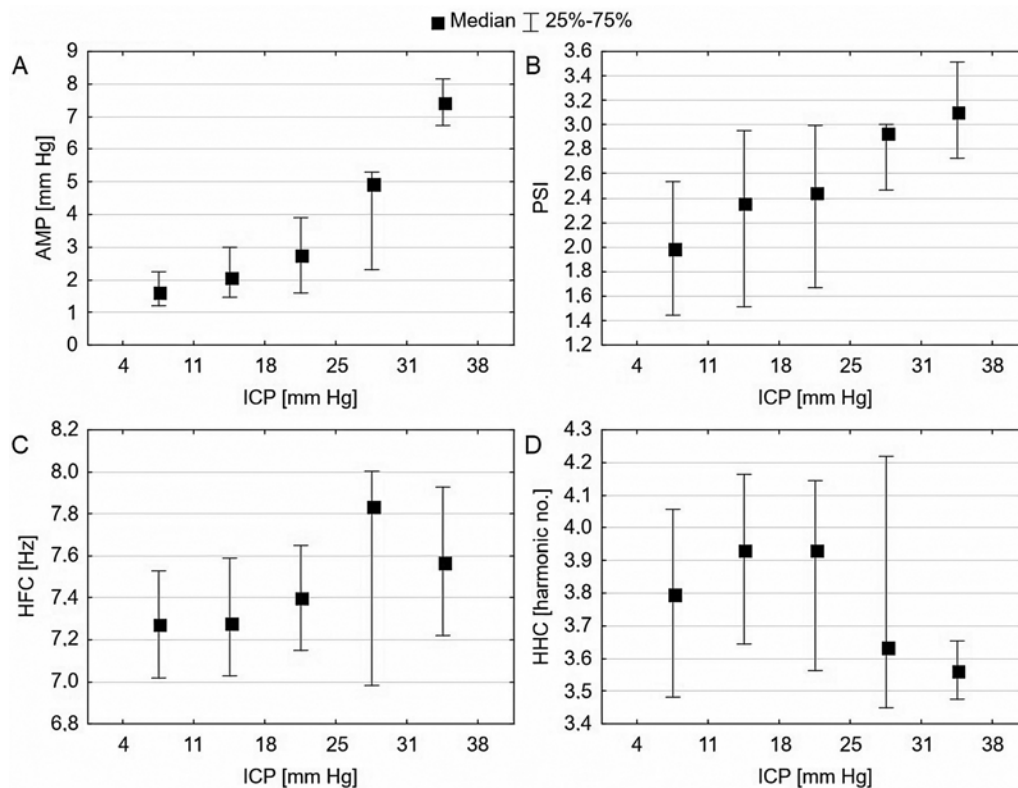


**FIG. 3.** The relationship between mean ICP and ICP pulse waveform–derived parameters. **A:** AMP of ICP. **B:** PSI. **C:** HFC. **D:** HHC in the full group of TBI patients. Data are presented as median (black square) and IQR (whiskers).

higher in patients with HFC > 7.60 Hz ( $F = 3.53, p < 0.001$ ) (Fig. 5B).

PSI was significantly greater in deceased patients (median [IQR] 2.96 [2.36–3.07]) than in those who survived (2.13 [1.43–2.77],  $p < 0.001$ ), with medium effect size ( $r = 0.30$ ). Furthermore, PSI was a significant predictor of mortality (PSI cutoff value 2.34,  $AUC = 0.71, p < 0.001$ ). Based on the Kaplan-Meier survival analysis,  $PSI > 2.34$  increased the risk of death ( $F = 3.83, p < 0.001$ ) (Fig. 5C).

HHC was similar between patients who died and those who survived.

## Discussion

Earlier works have reported that changes in ICP pulse waveform indicate changes in cerebrospinal compliance and may be clinically useful for analysis along with the traditionally considered mean ICP value.<sup>5,10</sup> Although many parameters have been proposed for ICP pulse waveform analysis, they have never been compared in the same database. In this study, 2 spectral centroid metrics, as well as the amplitude and morphological shape of the ICP pulse waveform, were examined and compared in a multicenter cohort of TBI patients.

### Relationships Between ICP Pulse Waveform–Derived Parameters and Mean ICP

Both the HHC versus mean ICP and HFC versus mean ICP plots demonstrated breakpoints after which the pa-

rameters ceased to increase, but HHC started to decline at a lower ICP level than HFC. HFC was almost linearly related to increasing ICP to its high value around 31 mm Hg and then decreased, whereas HHC was nonlinearly dependent on increasing ICP and demonstrated a breakpoint at an ICP level of about 25 mm Hg. These findings are in line with previously reported results.<sup>11–13</sup> Earlier stud-

**TABLE 2.** ICP and derived parameters, arterial blood pressure, and heart rate with regard to the presence or absence of MLS in early CT scans (first scan after hospital admission)

Parameter	MLS in Early CT Scan	
	Present (n = 39)	Absent (n = 123)
ICP, mm Hg	15.29 (5.40)	12.09 (7.14)*
AMP, mm Hg	2.11 (1.80)	2.01 (1.57)
PSI, AU	3.00 (1.14)	2.16 (1.23)†
HFC, Hz	7.54 (0.57)	7.25 (0.51)†
HHC, harmonics no.	4.13 (0.54)	3.81 (0.52)*
ABP, mm Hg	85.00 (13.42)	82.66 (12.11)
HR, bpm	72.16 (20.28)	74.57 (19.29)

Values are shown as median (IQR). Information about MLS was unavailable for 22 patients.

\*  $p < 0.01$ .

†  $p < 0.001$ .

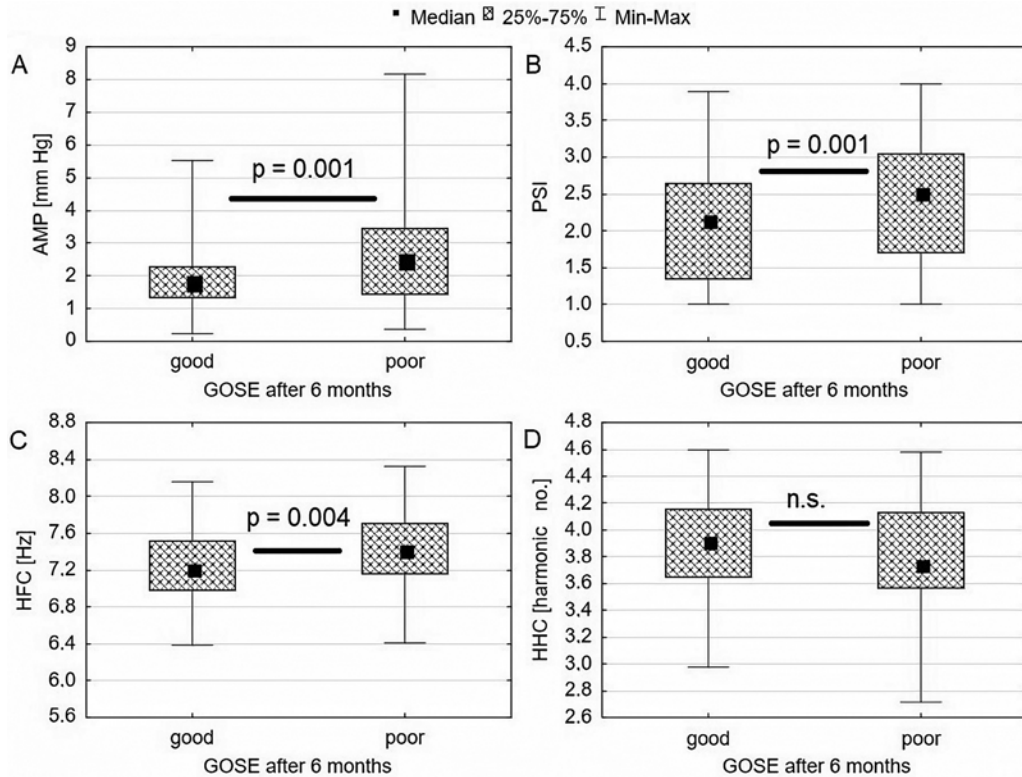


**FIG. 4.** Differences in AMP of ICP (A), PSI (B), HFC (C), and HHC (D) between the good and poor outcome groups based on GOSE score after 6 months. Data are shown as median (central black squares), IQR (gray boxes), and range (whiskers). n.s. = not statistically significant.

ies showed that HFC increases with transient intracranial hypertension and during plateau waves<sup>22</sup> but decreases during refractory intracranial hypertension.<sup>23</sup> For the first time, Zakrzewska et al. demonstrated that HHC decreases and the breakpoint in the ICP-HHC characteristic exists during plateau waves.<sup>13</sup> These findings suggest that HHC could predict risk of intracranial hypertension, whereas HFC may be an early indicator of critically high ICP associated with diminished cerebral blood flow and risk of ischemia. This observation requires further studies for confirmation; however, the topic may spark some research interest based on these results.

**Association With Mortality and Outcome**

We found that HFC, PSI, and AMP—but not HHC—

were associated with mortality and outcome 6 months after TBI. Moreover, based on the results of the survival analysis, we showed that mean AMP, PSI, and HFC significantly differentiated between deceased and surviving patients. The probability of survival after 6 months decreased by about 60% if the mean values of these parameters (estimated during the first 7 days after injury) were greater than the proposed threshold values. The mean value of HHC did not significantly distinguish between outcome or survival. The associations of AMP, HFC, and PSI with mortality and outcome have been previously reported,<sup>9,10</sup> but we are unaware of any study that assessed the correlation between outcome and HHC. The reason why HHC did not correlate with outcome may be related to the fact that it was the only parameter that showed a nonlin-

**TABLE 3. Comparison of ICP-derived metrics with GOSE scores in subgroups with low ICP (< 15 mm Hg) and high ICP (≥ 15 mm Hg), where good outcome is defined as GOSE score 5–8 and poor outcome as GOSE score 1–4**

Metric	ICP <15 mm Hg			ICP ≥15 mm Hg		
	Good Outcome	Poor Outcome	p Value	Good Outcome	Poor Outcome	p Value
HFC, Hz	7.21 (0.51)	7.40 (0.46)	<b>0.022</b>	7.24 (0.52)	7.45 (0.62)	0.150
HHC, harmonics no.	3.84 (0.55)	3.71 (0.48)	0.285	4.04 (0.41)	3.87 (0.57)	0.197
PSI, AU	1.82 (1.36)	2.48 (1.43)	<b>0.005</b>	2.46 (0.68)	2.73 (1.13)	0.224
AMP, mm Hg	1.69 (0.75)	2.24 (1.57)	<b>0.007</b>	2.30 (0.75)	3.00 (2.90)	0.154

Values are shown as median (IQR) unless indicated otherwise. Boldface type indicates statistical significance (p < 0.05).



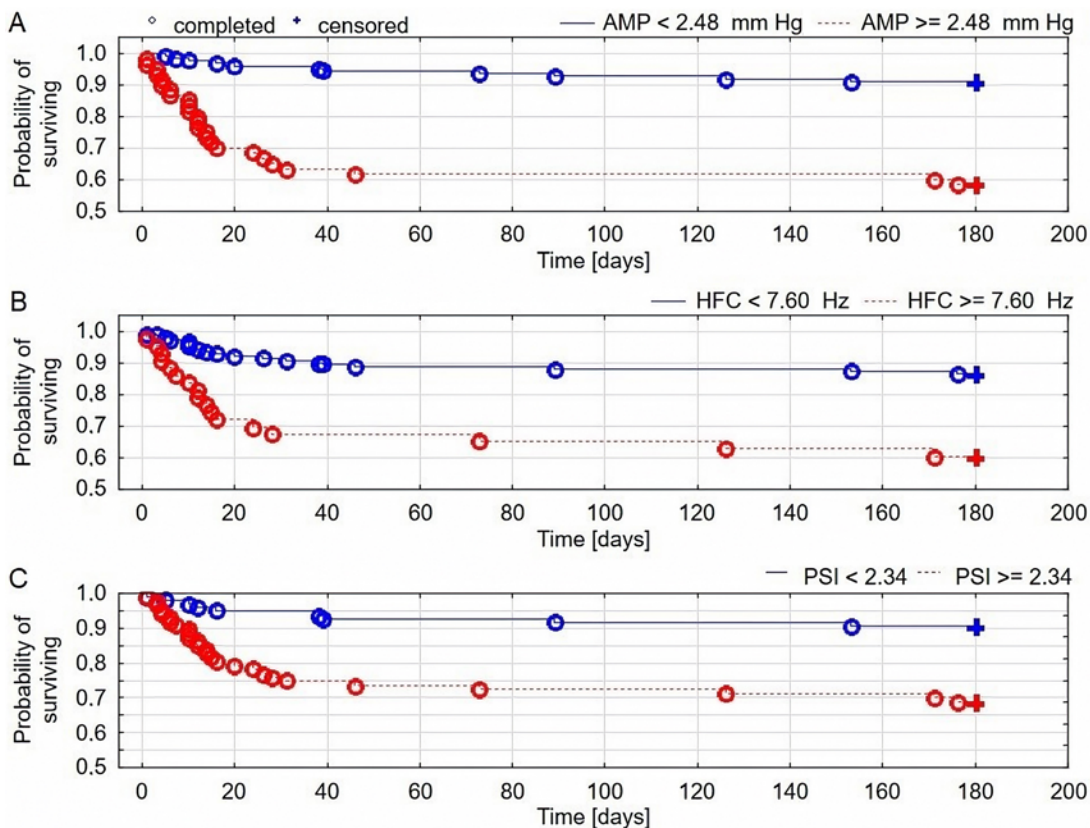


**FIG. 5.** Kaplan-Meier plots showing probability of survival based on the thresholds of AMP of ICP (A), HFC (B), and PSI (C). The solid blue line reflects the probability of survival among patients with a favorable ICP-derived index, whereas the dotted red line marks the probability of survival among patients with a poor ICP-derived index. Figure is available in color online only.

ear dependence on changes in mean ICP. PSI, AMP, and HFC—but not HHC—were significantly greater in patients with low mean ICP (< 15 mm Hg) and poor outcome. This supports the clinical utility of using ICP pulse waveform analysis in addition to mean ICP. Furthermore, PSI, HFC, and HHC were related to the appearance of MLS, which is associated with elevated ICP and increased morbidity and mortality.<sup>24</sup>

### Limitations

Despite the interesting preliminary results, some limitations should be emphasized. First, the ICP pulse waveform-derived parameters analyzed in this paper were not stratified according to clinical condition of the patients, cause of brain damage, or admission CT scores. We did not include the RAP index<sup>25</sup> or the cerebral pressure reactivity index (PRx)<sup>26</sup> in the main analysis in order to limit the number of considered parameters and to clarify the evaluations of the various interrelationships. However, the relationships between RAP, PRx, and ICP pulse waveform-derived parameters should be considered in further studies. Furthermore, we evaluated only admission CT scans in the MLS analysis and did not comment on the association between CT changes over time and ICP-derived parameters. Second, in this study, we analyzed only the relationship between ICP shape-derived parameters and patient outcomes. We did not build an advanced predic-

tion model. However, the next step of this work will be devoted to the development of a model for the prediction of treatment results in TBI patients that uses an artificial neural network and is based on both demographic data and parameters obtained from physiological signals, including the shape of ICP pulsations. This was beyond the scope of the current study because this is a highly complex predictive task. Third, automation of ICP pulse waveform annotations eliminates operator bias and makes categorization accessible to clinical staff; however, the clinical relevance and objectiveness of ICP pulse waveform classification is still a matter of debate. Finally, because the presented results are from a retrospective analysis of monitoring data, a prospective confirmation study is required to conclusively prove the clinical utility of the analyzed metrics.

### Conclusions

Our results demonstrated that HFC, AMP, and PSI could potentially be applied as predictors of mortality after TBI and were associated with poor outcome even in patients with low ICP, whereas HHC has the potential to be used as an early indicator of impending intracranial hypertension in TBI patients. This study supports the importance of analyzing the ICP pulse waveform, in addition to recording mean ICP. Furthermore, analysis of ICP pulse waveform-derived metrics, in contrast to the measure-

ment of mean ICP values, remains immune to zero drift of the ICP sensor.

## Appendix

### CENTER-TBI High-Resolution Sub-Study Participants and Investigators

Audny Anke, MD, PhD,<sup>1</sup> Ronny Beer, MD,<sup>2</sup> Bo-Michael Bellander, MD, PhD,<sup>3</sup> Erta Beqiri, MD,<sup>4</sup> Andras Buki, MD, PhD,<sup>5</sup> Manuel Cabeleira, MSc,<sup>6</sup> Marco Carbonara, MD,<sup>7</sup> Arturo Chierogato, MD,<sup>4</sup> Giuseppe Citerio, MD,<sup>8,9</sup> Hans Clusmann, MD,<sup>10</sup> Endre Czeiter, MD, PhD,<sup>11</sup> Marek Czosnyka, PhD,<sup>6</sup> Bart Depreitere, MD, PhD,<sup>12</sup> Ari Ercole, MD, PhD,<sup>13</sup> Shirin Frisvold, MD, PhD,<sup>14</sup> Raimund Helbok, MD, PhD,<sup>2</sup> Stefan Jankowski, PhD,<sup>15</sup> Danile Kondziella, MD, PhD,<sup>16</sup> Lars-Owe Koskinen, MD, PhD,<sup>17</sup> Ana Kowark, MD,<sup>18</sup> David K. Menon, MD, PhD,<sup>13</sup> Geert Meyfroidt, MD, PhD,<sup>19</sup> Kirsten Moeller, MD, PhD,<sup>20</sup> David Nelson, MD, PhD,<sup>3</sup> Anna Piippo-Karjalainen, MD, PhD,<sup>21</sup> Andreea Radoi, PhD,<sup>22</sup> Arminas Ragauskas, PhD,<sup>23</sup> Rahul Raj, MD, PhD,<sup>21</sup> Jonathan Rhodes, MD,<sup>24</sup> Saulius Rocka, MD, PhD,<sup>23</sup> Rolf Rossaint, MD, PhD,<sup>18</sup> Juan Sahuquillo, MD, PhD,<sup>22</sup> Oliver Sakowitz, MD, PhD,<sup>25,26</sup> Peter Smielewski, PhD,<sup>6</sup> Nino Stocchetti, MD,<sup>27</sup> Nina Sundström, PhD,<sup>28</sup> Riikka Takala, MD, PhD,<sup>29</sup> Tomas Tamosiutis, MD, PhD,<sup>30</sup> Olli Tenovu, MD, PhD,<sup>31</sup> Andreas Unterberg, MD, PhD,<sup>26</sup> Peter Vajkoczy, MD, PhD,<sup>32</sup> Alessia Vargiolu, PhD,<sup>8</sup> Rimantas Vilcinis, MD, PhD,<sup>33</sup> Stefan Wolf, MD, PhD,<sup>34</sup> Alexander Younsi, MD,<sup>26</sup> and Frederick A. Zeiler, MD, PhD, CIP.<sup>13,35</sup>

<sup>1</sup>Department of Physical Medicine and Rehabilitation, University Hospital Northern Norway, Tromsø, Norway; <sup>2</sup>Department of Neurology, Neurological Intensive Care Unit, Medical University of Innsbruck, Innsbruck, Austria; <sup>3</sup>Department of Neurosurgery & Anesthesia & Intensive Care Medicine, Karolinska University Hospital, Stockholm, Sweden; <sup>4</sup>NeuroIntensive Care, Niguarda Hospital, Milan, Italy; <sup>5</sup>Department of Neurosurgery, Medical School, University of Pécs, Hungary, and Neurotrauma Research Group, János Szentágotthai Research Centre, University of Pécs, Hungary; <sup>6</sup>Brain Physics Lab, Division of Neurosurgery, Department of Clinical Neurosciences, University of Cambridge, Addenbrooke's Hospital, Cambridge, United Kingdom; <sup>7</sup>Neuro ICU, Fondazione IRCCS Cà Granda Ospedale Maggiore Policlinico, Milan, Italy; <sup>8</sup>NeuroIntensive Care Unit, Department of Anesthesia & Intensive Care, ASST di Monza, Monza, Italy; <sup>9</sup>School of Medicine and Surgery, Università Milano Bicocca, Milano, Italy; <sup>10</sup>Department of Neurosurgery, Medical Faculty RWTH Aachen University, Aachen, Germany; <sup>11</sup>Department of Neurosurgery, University of Pécs and MTA-PTE Clinical Neuroscience MR Research Group and Janos Szentágotthai Research Centre, University of Pécs, Hungarian Brain Research Program (grant no. KTIA 13 NAP-A-II/8), Pécs, Hungary; <sup>12</sup>Department of Neurosurgery, University Hospitals Leuven, Leuven, Belgium; <sup>13</sup>Division of Anaesthesia, University of Cambridge, Addenbrooke's Hospital, Cambridge, United Kingdom; <sup>14</sup>Department of Anesthesiology and Intensive Care, University Hospital Northern Norway, Tromsø, Norway; <sup>15</sup>Neurointensive Care, Sheffield Teaching Hospitals NHS Foundation Trust, Sheffield, United Kingdom; <sup>16</sup>Departments of Neurology, Clinical Neurophysiology, and Neuroanesthesiology, Region Hovedstaden Rigshospitalet, Copenhagen, Denmark; <sup>17</sup>Department of Clinical Neuroscience, Neurosurgery, Umeå University, Umeå, Sweden; <sup>18</sup>Department of Anaesthesiology, University Hospital of Aachen, Aachen, Germany; <sup>19</sup>Intensive Care Medicine, University Hospitals Leuven, Leuven, Belgium; <sup>20</sup>Department of Neuroanesthesiology, Region Hovedstaden Rigshospitalet, Copenhagen, Denmark; <sup>21</sup>Helsinki University Central Hospital, Helsinki, Finland; <sup>22</sup>Department of Neurosurgery, Vall d'Hebron University Hospital, Barcelona, Spain; <sup>23</sup>Department of Neurosurgery, Kaunas University of Technology and Vilnius University, Vilnius, Lithuania;

<sup>24</sup>Department of Anaesthesia, Critical Care & Pain Medicine NHS Lothian & University of Edinburgh, Edinburgh, United Kingdom; <sup>25</sup>Klinik für Neurochirurgie, Klinikum Ludwigsburg, Ludwigsburg, Germany; <sup>26</sup>Department of Neurosurgery, University Hospital Heidelberg, Heidelberg, Germany; <sup>27</sup>Department of Pathophysiology and Transplantation, Milan University, and Neuroscience ICU, Fondazione IRCCS Cà Granda Ospedale Maggiore Policlinico, Milano, Italy; <sup>28</sup>Department of Radiation Sciences, Biomedical Engineering, Umeå University, Umeå, Sweden; <sup>29</sup>Perioperative Services, Intensive Care Medicine, and Pain Management, Turku University Central Hospital and University of Turku, Turku, Finland; <sup>30</sup>Neuro-Intensive Care Unit, Kaunas University of Health Sciences, Kaunas, Lithuania; <sup>31</sup>Rehabilitation and Brain Trauma, Turku University Central Hospital and University of Turku, Turku, Finland; <sup>32</sup>Neurologie, Neurochirurgie und Psychiatrie, Charité-Universitätsmedizin Berlin, Berlin, Germany; <sup>33</sup>Department of Neurosurgery, Kaunas University of Health Sciences, Kaunas, Lithuania; <sup>34</sup>Department of Neurosurgery, Charité-Universitätsmedizin Berlin, corporate member of Freie Universität Berlin, Humboldt-Universität zu Berlin, and Berlin Institute of Health, Berlin, Germany; and <sup>35</sup>Section of Neurosurgery, Department of Surgery, Rady Faculty of Health Sciences, University of Manitoba, Winnipeg, Manitoba, Canada.

## Acknowledgments

We thank Marek Skarupski, PhD, from the Faculty of Pure and Applied Mathematics, Wrocław University of Science and Technology, Wrocław, Poland, for his helpful comments and for reviewing the statistical methodology used in our study. This work was supported by the National Science Centre, Poland (grant no. UMO-2019/35/B/ST7/00500). Dr. Czosnyka is supported by the National Institute for Health Research and MIC (Biomedical Research Centre Cambridge, United Kingdom).

## References

- Batson C, Stein KY, Gomez A, et al. Intracranial pressure-derived cerebrovascular reactivity indices, chronological age, and biological sex in traumatic brain injury: a scoping review. *Neurotrauma Rep.* 2022;3(1):44-56.
- Czosnyka M, Smielewski P, Timofeev I, et al. Intracranial pressure: more than a number. *Neurosurg Focus.* 2007;22(5):E10.
- Hu X, Glenn T, Scalzo F, et al. Intracranial pressure pulse morphological features improved detection of decreased cerebral blood flow. *Physiol Meas.* 2010;31(5):679-695.
- Kasprowicz M, Lalou DA, Czosnyka M, Garnett M, Czosnyka Z. Intracranial pressure, its components and cerebrospinal fluid pressure-volume compensation. *Acta Neurol Scand.* 2016;134(3):168-180.
- Cardoso ER, Rowan JO, Galbraith S. Analysis of the cerebrospinal fluid pulse wave in intracranial pressure. *J Neurosurg.* 1983;59(5):817-821.
- Heldt T, Zoerle T, Teichmann D, Stocchetti N. Intracranial pressure and intracranial elastance monitoring in neurocritical care. *Annu Rev Biomed Eng.* 2019;21:523-549.
- Szewczykowski J, Sliwka S, Kunicki A, Dytko P, Korsak-Sliwka J. A fast method of estimating the elastance of the intracranial system. *J Neurosurg.* 1977;47(1):19-26.
- Czosnyka M, Guazzo E, Whitehouse M, et al. Significance of intracranial pressure waveform analysis after head injury. *Acta Neurochir (Wien).* 1996;138(5):531-542.
- Zeiler FA, Ercole A, Cabeleira M, et al. Compensatory-reserve-weighted intracranial pressure versus intracranial pressure for outcome association in adult traumatic brain injury: a CENTER-TBI validation study. *Acta Neurochir (Wien).* 2019;161(7):1275-1284.

10. Radolovich DK, Aries MJH, Castellani G, et al. Pulsatile intracranial pressure and cerebral autoregulation after traumatic brain injury. *Neurocrit Care*. 2011;15(3):379-386.
11. Robertson CS, Narayan RK, Contant CF, et al. Clinical experience with a continuous monitor of intracranial compliance. *J Neurosurg*. 1989;71(5 Pt 1):673-680.
12. Berdyga J, Czosnyka M, Czernicki Z, Williamson M. Analysis of the intracranial pressure waveform by means of spectral methods. In: Avezaat CJJ, Eijndhoven JHM, Maas AIR, Tans JTJ, eds. *Intracranial Pressure VIII*. Springer; 1993: 372-375.
13. Zakrzewska AP, Placek MM, Czosnyka M, Kasprowicz M, Lang EW. Intracranial pulse pressure waveform analysis using the higher harmonics centroid. *Acta Neurochir (Wien)*. 2021;163(12):3249-3258.
14. Mataczynski C, Kazimierska A, Uryga A, Burzynska M, Rusiecki A, Kasprowicz M. End-to-end automatic morphological classification of intracranial pressure pulse waveforms using deep learning. *IEEE J Biomed Health Inform*. 2022; 26(2):494-504.
15. Kazimierska A, Uryga A, Mataczynski C, et al. Analysis of the shape of intracranial pressure pulse waveform in traumatic brain injury patients. *Annu Int Conf IEEE Eng Med Biol Soc*. 2021;2021:546-549.
16. Czosnyka M, Czosnyka Z. Origin of intracranial pressure pulse waveform. *Acta Neurochir (Wien)*. 2020;162(8):1815-1817.
17. Carney NA, Ghajar J. Guidelines for the management of severe traumatic brain injury. Introduction. *J Neurotrauma*. 2007;24(suppl 1):S1-S106.
18. Chopp M, Portnoy HD. Systems analysis of intracranial pressure. Comparison with volume-pressure test and CSF-pulse amplitude analysis. *J Neurosurg*. 1980;53(4):516-527.
19. Nucci CG, De Bonis P, Mangiola A, et al. Intracranial pressure wave morphological classification: automated analysis and clinical validation. *Acta Neurochir (Wien)*. 2016;158(3): 581-588.
20. Bishop SM, Ercole A. Multi-scale peak and trough detection optimised for periodic and quasi-periodic neuroscience data. *Acta Neurochir Suppl*. 2018;126:189-195.
21. Beslow LA, Licht DJ, Smith SE, et al. Predictors of outcome in childhood intracerebral hemorrhage: a prospective consecutive cohort study. *Stroke*. 2010;41(2):313-318.
22. Robertson CS, Contant CF, Narayan RK, Grossman RG. Comparison of methods for ICP waveform analysis with intracranial hypertension in head-injured patients. In: Avezaat CJJ, Eijndhoven JHM, Maas AIR, Tans JTJ, eds. *Intracranial Pressure VIII*. Springer; 1993:348-355.
23. Contant CF Jr, Robertson CS, Crouch J, Gopinath SP, Narayan RK, Grossman RG. Intracranial pressure waveform indices in transient and refractory intracranial hypertension. *J Neurosci Methods*. 1995;57(1):15-25.
24. Puffer RC, Yue JK, Mesley M, et al. Long-term outcome in traumatic brain injury patients with midline shift: a secondary analysis of the Phase 3 COBRIT clinical trial. *J Neurosurg*. 2018;131(2):596-603.
25. Czosnyka M, Steiner L, Balestreri M, et al. Concept of "true ICP" in monitoring and prognostication in head trauma. *Acta Neurochir Suppl*. 2005;95(95):341-344.
26. Czosnyka M, Smielewski P, Kirkpatrick P, Laing RJ, Menon D, Pickard JD. Continuous assessment of the cerebral vasomotor reactivity in head injury. *Neurosurgery*. 1997;41(1): 11-19.

---

## Disclosures

The authors report no conflict of interest concerning the materials or methods used in this study or the findings specified in this paper.

## Author Contributions

Conception and design: Uryga, Kazimierska, Pudełko, Mataczyński, Lang, Czosnyka, Kasprowicz. Analysis and interpretation of data: all authors. Drafting the article: Uryga, Ziółkowski, Kazimierska, Czosnyka, Kasprowicz. Critically revising the article: Uryga, Pudełko, Mataczyński, Lang, Kasprowicz. Reviewed submitted version of manuscript: Czosnyka. Study supervision: Czosnyka, Kasprowicz.

## Supplemental Information

### Online-Only Content

Supplemental material is available with the online version of the article.

*Supplementary Data*. <https://thejns.org/doi/suppl/10.3171/2022.10.JNS221523>.

## Correspondence

Agnieszka Uryga: Wrocław University of Science and Technology, Wrocław, Poland. [agnieszka.uryga@pwr.edu.pl](mailto:agnieszka.uryga@pwr.edu.pl).